

# The Lateral Distribution Function of Extensive Air Showers Measured by Maket-ANI detector

G. Hovsepyan<sup>a</sup>, A. Chilingarian<sup>a</sup>, G. Gharagyozyan<sup>a</sup>, S. Ghazaryan<sup>a</sup>, E. Mamijanyan<sup>a,b</sup> and L. Melkumyan<sup>a</sup>

(a) Cosmic Ray Division, Yerevan Physics Institute, Alikhanyan Brothers 2, Yerevan 36, Armenia

(b) Moscow Lebedev Institute, Leninsky pr.56, Moscow 117924, Russia

Presenter: G.Hovsepyan (hgg@crdlx5.yerphi.am), arm-hovsepyan-G-abs2-he12-poster

The MAKET-ANI detector is operating at altitude 3200 m., at slope of mt. Aragats in Armenia. More than million showers with size, greater than  $10^5$  were registered, by the MAKET-ANI detector in 1999-2004. Detector has effectively collected the cores of EAS, initiated by primaries with energies of  $5 \cdot 10^{14}$  -  $3 \cdot 10^{17}$  eV. After proving that the quality of the reconstruction of the Extensive Air Showers (EAS) size and shape are reasonably good we present the LDF functions for the distances up to 120 m. from EAS core. The obtained LDF functions are compared with CORSIKA562 (QGSJET, NKG) [1,2] simulations. Proceeding from the dependences of shower age on shower size we discuss the mass composition models supported by experimental evidence.

## 1. Introduction

The MAKET-ANI surface array [3,4] consists of 92 particle density detectors formed from plastic scintillators with thickness of 5 cm. Twenty four of them have area  $0.09 \text{ m}^2$  and 68 have area of  $1 \text{ m}^2$ . The central part consists of 73 scintillation detectors and is arranged in a rectangle of  $85 \times 65 \text{ m}^2$ . Two peripheral points of a distance of 95m and 65m from the center of the installation consist of 15 and 4 scintillators respectively. In order to estimate the zenith and azimuth angles 19 detectors from 92 (with area  $1 \text{ m}^2$ ) are equipped with timing readout measuring the EAS front appearance with an accuracy of  $\sim 5 \text{ ns}$ . The photomultipliers (PM-49) are placed in light-tight iron boxes. Logarithmic amplitude-digital converters (ADC) and constant fraction discriminators (CFD) are assembled just above PM. The dynamic range of the registered particle number is  $\sim 5 \times 10^3$ .

The normalization from PM amplitude to number of particles is performed by calibration spectrum with mode equal to 11 MeV. The transition from “scintillation” densities to “electronic” ones is made by [5]:  $\rho_{sc}(r)/\rho_e(r) = (r/R_M)^\alpha$ , where  $\alpha = -0.18$  and  $R_M$  is Molier radii.

The Nishimura-Kamata Greizen approximation is used for Extensive Air Shower (EAS) characteristic estimation [6]:

$$\rho_e(r) = \frac{N_e}{2 \cdot \pi \cdot R_M^2} \cdot C(s) \cdot \left(\frac{r}{R_M}\right)^{(s-2)} \cdot \left(\frac{r}{R_M} + 1\right)^{(s-4.5)}, \quad (1)$$

where  $\rho_e(r)$  - is the particle density on the distance  $r$  from shower axes,  $N_e$  - total number of shower electrons,  $R_M = 118 \text{ m}$  - Molier radii,  $s$  - shower age parameter and  $C(s) = 0.366 s^2 (2.07-s)^{1.25}$  [7].

The uncertainties of the reconstruction of EAS parameters are as following: shower size  $\Delta N_e \sim 10\%$ , the shower shape (age) parameter -  $\Delta s \sim 0.06$ . The accuracies of EAS angles determination are:  $\Delta \theta \sim 1.5^\circ$  and  $\Delta \phi < 5^\circ$  [8].

Monte-Carlo calculations with CORSIKA562 (QGSJET, NKG) confirmed that EAS with sizes  $N_e > 5 \cdot 10^4$  and core, located within the rectangle of  $20 \times 44 \text{m}^2$ , are selected with efficiency  $\varepsilon \geq 95\%$ . Showers are initiated by primary ions with energies greater than  $3 \cdot 10^6 \text{ GeV}$  (see Figure1).

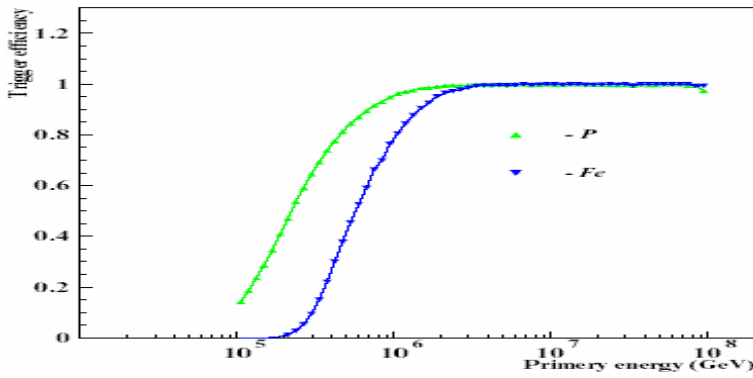


Figure 1. Efficiency of the MAKET-ANI detector for the showers localized in area of  $(20 \times 44) \text{ m}^2$

## 2. The Lateral Distribution Function (LDF) of shower particles.

In the period of 1998 - 2004 approximately  $1.2 \cdot 10^7$  showers were registered with effective registration time of about  $1.34 \cdot 10^8 \text{ sec}$ . From these showers  $\sim 1,200,000$  events only were selected for the further treatment. We selected EAS cores from more compact area around the geometrical center of MAKET-ANI detector, ensuring high efficiency of EAS registration. The following cuts were applied for the events selection:  $N_e > 10^5$ ,  $0.3 < s < 1.7$ , core position within area providing efficiency  $\varepsilon \geq 95\%$ ,  $\theta < 46.8^\circ$ . The LDF functions were estimated in the 5 zenith angle intervals, uniformly distributed according to  $\text{Sec}(\theta)$  and in logarithmic uniform intervals distributed according to  $N_e$  ( $\Delta \text{Lg}(N_e) = 0.3$ ). The distribution of the discrepancies (biases) between densities estimated by formula (1) and measured densities for all detector locations were calculated. The accuracy of the approximation function (1) turns out not worse than  $\pm 5\%$  [9].

In the Table 1 the “averaged” and approximated shower parameters are presented for the near vertical ( $\theta \leq 23.8^\circ$ ) showers. First 4 columns of Table 1 contain number of used showers, mean logarithm of shower size, mean age parameter and MSD of age. In the next columns the same averaged parameters, but obtained with approximation of LDF, are posted. Till shower sizes up to  $N_e = 10^{6.3}$  the approximation parameters fit the data very well, for larger shower sizes we exclude from approximation procedures detectors at near distances to avoid saturation effects.

Table 1. Comparison of measured and approximated by NKG function LDF .

| N                 | $\text{Lg}N_e^{\text{exp}}$ | $s^{\text{exp}}$ | $\sigma_s$ | $\text{Lg}N_e^{\text{LDF}}$ | $s^{\text{LDF}}$ | $\sigma_s^{\text{LDF}}$ |
|-------------------|-----------------------------|------------------|------------|-----------------------------|------------------|-------------------------|
| $3.78 \cdot 10^5$ | 5.15                        | 0.96             | 0.16       | 5.11                        | 0.98             | 0.14                    |
| $1.49 \cdot 10^5$ | 5.44                        | 0.92             | 0.14       | 5.44                        | 0.93             | 0.10                    |
| $5.98 \cdot 10^4$ | 5.74                        | 0.90             | 0.13       | 5.75                        | 0.90             | 0.05                    |
| $2.75 \cdot 10^4$ | 6.04                        | 0.89             | 0.12       | 6.04                        | 0.88             | 0.04                    |
| $1.08 \cdot 10^4$ | 6.33                        | 0.88             | 0.11       | 6.34                        | 0.86             | 0.04                    |
| $3.27 \cdot 10^3$ | 6.63                        | 0.88             | 0.11       | 6.65                        | 0.85             | 0.03                    |
| $8.83 \cdot 10^2$ | 6.93                        | 0.89             | 0.11       | 6.96                        | 0.84             | 0.03                    |
| $2.70 \cdot 10^2$ | 7.22                        | 0.91             | 0.11       | 7.26                        | 0.85             | 0.02                    |

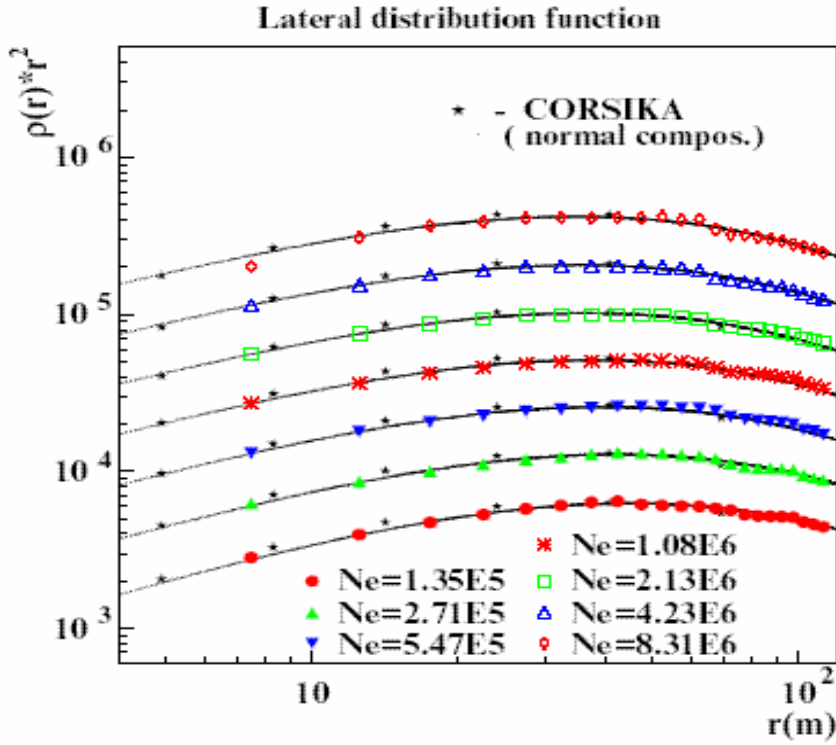


**Figure 2.** Observed LDF functions in comparison with simulated by CORSIKA 562(QGSJET, NKG).

In Figure 2 near vertical ( $\theta \leq 23.8^\circ$ ) LDF functions, measured in 7  $N_e$  intervals, are presented. The simulated LDF are noted by asterisks. Detector response function was calculated using CORSIKA simulations.  $2 \cdot 10^6$  events for each of 5 primary nuclei (H, He, O, Si, Fe) in the zenith angle range of  $0-50^\circ$ , for height of  $700 \text{ g/cm}^2$ , for energy starting from  $10^{14} \text{ eV}$  were simulated. Shower particles were followed till thresholds  $3 \text{ MeV}$  for electrons;  $50 \text{ MeV}$  for muons,  $100 \text{ MeV}$  for hadrons. Energy spectra has index  $\gamma_1 = -2.7$ , before knee and  $\gamma_2 = -3.1$  after knee for all nuclei. The knee position was simulated according to  $E_{\text{knee}} = Z \cdot E_0$ ,  $E_0 = 3 \cdot 10^{15} \text{ eV}$ ,  $Z$  is the charge of primary nuclei. The mass composition was taken as “normal” (36% H, 25% He, 14% O, 15% Si, 10% Fe) [10]. Simulated events undergo all procedures of experimental data analysis. Remarkable agreement of experimental and simulated LDF functions pointed on the correct treatment of transition effects in the scintillators.

### 3. Discussion

In Figure 3 we present the experimental dependence of age parameter on shower size in comparison with simulations for pure proton and iron composition. To compare experimental dependence with models we consider following possibilities:

1. “Normal” composition (36%P,25%He,14%O,15%Si,10%Fe) [10], knee position  $E_{\text{knee}} = Z \cdot 3 \cdot 10^{15} \text{ eV}$  - red solid;
2. “Normal” composition with fixed knee position  $E_{\text{knee}} = 3 \cdot 10^{15} \text{ eV}$  for all nuclei - red dashed;
3. “Heavy” composition (5%P,5%He,10%O,10%Si,70% Fe) [11], knee position  $E_{\text{knee}} = Z \cdot 3 \cdot 10^{15} \text{ eV}$  - green.

As we see from the Figure 3 first option fits experimental data rather well, therefore we can exclude options 2 and 3.

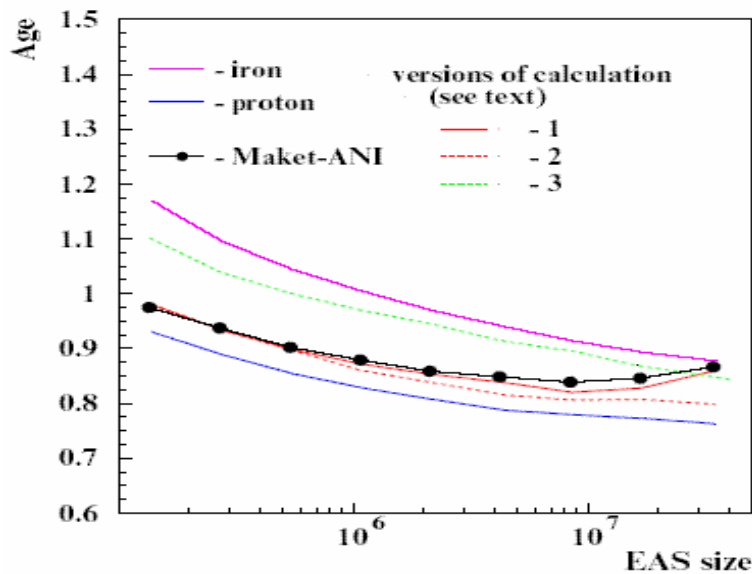


Figure 3. Dependence of the averaged shower shape (age) parameter on shower size

#### 4. Acknowledgements

We thank the staff of Aragats Mountain Cosmic Ray Observatory for help in operation of Maket-ANI experiment. We thank also ANI collaboration members for their fruitful cooperation over many years. This work was supported by Armenian government grant, by ISTC grant A – 1058.

#### References

- [1] D.Heck et al. FZKA report 6019, Forschungszentrum, Karlsruhe (1998)
- [2] N.Kalmikov, S.Ostapchenko, A. Pavlov Nucl.Phis.B. (Proc.Suppl.), 52B, 17 (1997)
- [3] E.Bazarov et al. Voprosy Atomnoi Nauki i Tekhniki.(VANI T) ser.Nucl.Phis.Reser. ,v.5(31), p.3-16 (in Russian) .G. Gharagozyan for the ANI collab., Proc. of the Workshop ANI98, FZKA 6215, Forschungszentrum Karlsruhe, (1998)
- [4] A.Chilingarian A. et al., Proc. 26-th ICRC , Salt Lake City, 240 (1999)  
A.Chilingaryan et al. Astrophys. Jour., 603, L29-L32 (2004)
- [5] S.Blokhin , V.Romakhin , G.Hovsepyan Proc. Workshop ANI 99, Nor-Amberd (1999)
- [6] K.Kamata, J.Nishimura, Progr. Theoret. Phys., Supp. 93 (1958)
- [7] S. Hayakawa, Cosmic Ray Physics, Interscience Monographs and Texts in Physics and Astronomy, 22, Wiley-Interscience, (1969)
- [8] A.Chilingarian, G. Gharagozyan, H. Martirosyan Proc. 27-th ICRC, Hamburg, v. 2 p. 590 (2001)
- [9] S.Blokhin et al. to be published, Izv.AN RF, Phys.,(in Russian, 28-th RCRC)
- [10] G.B.Khristiansen et al. Astropart. Physics,2 , 127-136 (1994)
- [11] E.Juliusson 13-th ECRC, Geneva, OG-6.11 (1993)